

Statistical dynamics of dislocations in simple models of plastic deformation: Phase transitions and related phenomena

M.-Carmen Miguel^{a,*}, Paolo Moretti^b, Michael Zaiser^b, Stefano Zapperi^c

^a *Departament de Física Fonamental, Facultat de Física, Universitat de Barcelona, Diagonal 647, E-08028 Barcelona, Spain*

^b *Center for Materials Science and Engineering, University of Edinburgh, King's Buildings, Sanderson Building, Edinburgh EH9 3JL, UK*

^c *INFN UdR Roma 1 and SMC, Dipartimento di Fisica, Università "La Sapienza", P.le A. Moro 2, 00185 Roma, Italy*

Received in revised form 30 December 2004; accepted 1 March 2005

Abstract

Dislocation assemblies in crystalline substrates are a beautiful example of the broad class of systems that are governed by the presence of kinematical constraints induced by interactions, geometry, and/or disorder. The interactions between dislocation lines of different type together with the dynamic constraints which tie the motion of the dislocations to their slip planes lead to the possibility of forming metastable jammed configurations even in the absence of any disorder in the material. However, general dislocation assemblies will also be affected by the presence of disorder-induced pinning forces. In this paper we study several aspects concerning the dynamics of dislocation assemblies in simple models of plastic deformation that we believe we can successfully address with the conceptual and technical tools provided by Statistical Mechanics. In particular, we discuss the yielding (or jamming) transition between stationary and moving states in these models, the intermittent and globally slow relaxations observed around this transition, and the stress–strain relationships measured in the steady regime of deformation. We also briefly describe the main implications of sample geometry and of quenched disorder in dislocation assemblies present in the vortex lattice of type II superconductors, where we obtain some of the statistical dynamic properties of experimental interest.

© 2004 Elsevier B.V. All rights reserved.

Keywords: Dislocations; Plastic deformation; Phase transitions

1. Introduction

Statistical treatment of experimental data and numerical models of materials undergoing plastic deformation reveal important features underlying this fundamental process, such as intermittency, avalanches, and scaling relations. These and some other interesting properties are ubiquitous in the non-equilibrium dynamics of a wide variety of physical systems, including amorphous matter (glasses, foams, gels, polymeric melts, and most recently granular media) and crystalline solids (including vortex lattices). The dynamics of this wide class of physical systems shares the fact that it is governed by the presence of kinematical constraints, induced by interactions, geometry, and/or disorder. For several decades, Statistical Mechanics has been trying to offer a comprehensive

theory that is able to explain the thermodynamic and kinetic properties of some of these systems, both at the macroscopic and the mesoscopic level, and that is consistent with the wealth of experimental observations.

Dislocation assemblies in crystalline solids are yet another beautiful example of these broad class of systems, with several magnitudes playing a decisive role. The viscoplastic deformation of crystalline solids, including magnetic vortex lines in type II superconductors that naturally self-assemble into ordered arrays, is due to the creeping motion of dislocations driven by an externally applied stress [1–4]. Thus under stress conditions, both soft materials [5] and crystalline solids [6] are susceptible to display *jamming* and *shear yielding* that, in the case of soft-matter systems, is due to the interactions and spatial arrangement of their constituent particles, but in plastically deforming crystals is a consequence of the interactions and spatial arrangement of dislocations.

* Corresponding author.

E-mail address: carmen.miguel@ub.edu (M.-C. Miguel).

Over the last decade, decoration experiments in type II superconductors have provided new evidence regarding the important role of dislocations in the phase diagram of vortex matter. The Bitter decoration technique is a powerful method to investigate the topological properties of vortex matter by direct imaging. The vortex lattice structure is often observed to coexist with isolated dislocations, dipoles and grain boundaries. The latter are the signature of a vortex polycrystal with crystalline grains of different orientations [7]. Moreover, two-sided decoration experiments show that dislocations and grain boundaries usually thread the superconducting samples from top to bottom, i.e., one observes a columnar grain structure. This property guarantees that simplified dislocation dynamics models in two dimensions are appropriate to study the plastic phase of this non-conventional crystals, including dislocation mediated transitions. Much as in ordinary crystals, dislocations glide along their slip planes forming metastable jammed configurations. Dislocations and grain boundaries in the vortex lattice are also pinned by quenched disorder. The depinning transition of interacting dislocation assemblies in a random distribution of obstacles is a subject of great current interest, but it is of particular technological importance in vortex lattices. Besides, the elastic properties of vortex arrays depend on the magnetic field externally applied and can be easily tuned. This property makes this physical system particularly well suited for the study of grain growth mediated by grain boundary glide motion.

The paper is organized as follows: in section II we introduce jamming phenomena and discuss, in some detail, the jamming transition observed in plastically deformed crystals. In section III, we show that the onset of plastic flow in a superconducting disk occurs in correspondence with the nucleation and motion of new dislocations in the vortex lattice. In Section 4, we discuss the formation of a vortex polycrystal in type II superconductors from the competition between pinning and elastic forces. We also characterize the depinning current for grain boundaries in vortex lattices of various densities. Finally, in the last section we briefly summarize our main conclusions.

2. Dislocation jamming and viscoplastic creep deformation

In 1910 Andrade reported that the creep deformation of soft metals at constant temperature and stress grows in time according to a power law with exponent $1/3$, i.e. $\gamma \sim t^{1/3}$ where γ is the global strain of the material [8]. More generally, the creep deformation curve usually follows the relation $\gamma(t) = \gamma_0 + \beta t^{1/3} + \kappa t$, where γ_0 is the instantaneous plastic strain, $\beta t^{1/3}$ known as Andrade creep, and κt referred to as linear creep regime [1,2]. The same qualitative behavior has since been observed in many materials with rather different structures (including the creep compliance of amorphous polymer melts), leading to the conclusion that this should be a process determined by quite general principles, indepen-

dent of most material specific properties. Although there is still a lack of consensus on the basic mechanisms involved in the phenomenon, various arguments have been put forward within the dislocation literature [1,2,9–11] to try to explain Andrade's creep. Most of these arguments rely on thermally activated processes over time (or strain) dependent energy barriers.

As in the case of soft-matter systems, the plastic deformation of crystals only occurs when the externally applied stress overcomes a threshold value, the yield stress of the material. Above this threshold, large-scale dislocation motion may take place and a steady regime of plastic deformation is eventually established. Dislocations tend to move cooperatively under the action of external stress due to their mutual long-range and anisotropic elastic interactions, which can be attractive or repulsive. As a result of these interactions and the dislocation structures they give rise to, self-induced constraints build up in the system and the motion of dislocations may cease. Nevertheless, small variations of the external loading, the dislocation density and/or distribution, or the temperature, can enhance dislocation motion in a discontinuous and intermittent manner [12].

In Ref. [6], we studied the temporal relaxation of a relatively simple dislocation dynamics model through numerical simulation. In particular, a collection of parallel straight edge dislocations with Burgers vectors \mathbf{b}_i that can mutually annihilate and move in a single slip system under the action of constant stress was shown to give rise to Andrade-like creep at short and intermediate times for a wide range of applied stresses (see Ref. [13] for details regarding simulation units). We obtained such a result without invoking thermally activated processes, i.e. we considered an ideal situation where thermal fluctuations were irrelevant for the process (see Fig. 1). The strain rate, which is proportional to the density of mobile dislocations $d\gamma/dt = \sum_i b_i v_i$ with v_i the velocity of each dislocation, decays as a power law with an exponent close to $2/3$ in agreement with Andrade's

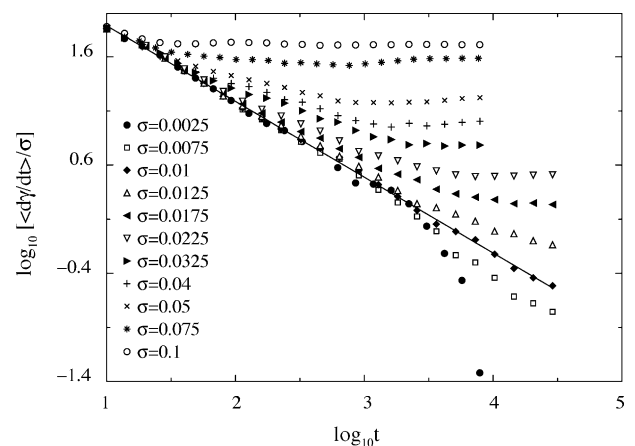


Fig. 1. Strain rate relaxation for different stress values [13]. The system size is $L = 100b$ and the initial density of edge dislocations is around 1%. The solid line is the best linear fit of the $\sigma = 0.01$ curve and yields $d\gamma/dt \sim t^{-0.69}$.

observations. At larger times, the strain-rate was observed to cross over to a linear creep regime (i.e. to a plateau signaling a steady rate of plastic deformation) whenever the applied stress is larger than a critical threshold σ_c , or, otherwise, to decay exponentially to zero.

These results suggest that a possible interpretation of dislocation motion and the corresponding creep laws of crystalline materials could also be found within the general “jamming” framework proposed for non-equilibrium soft and glassy materials [14,15]. Most of these physical systems consist of various types of soft particles closely packed into an amorphous state. At such high concentrations, the relative motion of these particles is drastically constrained and, as a consequence, they usually respond like elastic solids upon the application of low stresses. One then says that the system is jammed, since it is unable to explore all the available configuration space. On the other hand, they flow like viscous fluids above the so-called yield stress value σ_y , exhibiting a common rheology. Recent light scattering experiments [16,17] allow, for instance, to detect the intermittent dynamics of a gel formed from attractive colloids suggesting that intermittent behavior seems to be a fundamental ingredient for the slow relaxation of jammed materials. Moreover, this unjamming transition can be induced by changing either the external stress applied, the density, or the temperature of the system. The analogies of dislocation motion and these so-called jammed systems are further explored by considering the influences of dislocation multiplication, and thermal-like fluctuations on the dynamics. Dislocation multiplication favors the rearrangements of the system and induces a linear creep regime (flowing phase) at lower stress values, but it does not affect the initial power-law creep. The introduction of a finite effective temperature T has a similar effect [6].

The detailed analysis of the model data unveils the dislocation microscopic dynamics in the Andrade and the stationary regimes. Most dislocations are arranged into metastable structures so that the stress field generated in the material is screened out on large length-scales. These structures consist of small-angle dislocation boundaries separating slightly misoriented crystalline blocks or far more complex dislocation arrangements. If the applied stress is below the yield threshold, dislocations are unable to explore the space of configurations looking for more favorable arrangements and they are, most of the time, trapped in metastable configurations, which induce a jamming of the system. Around the yield threshold, a small fraction of dislocations may, however, attain a higher mobility and provoke several intermittent rearrangements of the whole system in the course of time. The shear stresses generated by these unsettled dislocations conserve the initial long-range character and force the system to continue evolving in time, in a cooperative manner, to try to screen them out (or minimize the elastic energy) by exploring further more favorable arrangements.

In Fig. 2, we show the root-mean-square velocity $\langle v^2 \rangle^{1/2} = [\sum_i v_i^2 / N]^{1/2}$ of all the dislocations ($N \sim 100$ –150) present in a square cell of size $L = 100b$ as a func-

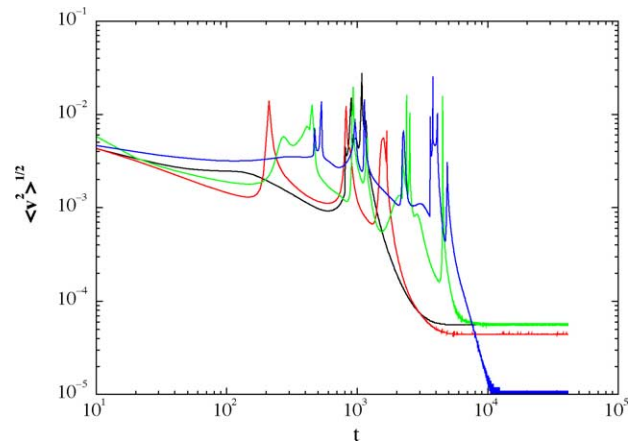


Fig. 2. Time evolution of the root-mean-square velocity of four simulation runs corresponding to different initial conditions. The applied stress is $\sigma = 0.0075$ in all cases [13]. The curves are depicted in a double logarithmic scale to emphasize the intermittent bursts characteristic of the creep dislocation dynamics around the yield threshold.

tion of time for four single runs of the numerical simulations. Thus, each run represents the creep behavior of a small piece (a few nanometers big) of a macroscopic system, and starts from four different initial dislocation configurations obtained after letting the system relax in the absence of external load during a given time interval. The external shear stress applied is in all cases $\sigma = 0.0075$, that is, in the vicinity of the critical threshold σ_c . We can clearly appreciate the presence of a few intermittent bursts after which $\langle v^2 \rangle^{1/2}$ slowly decreases in time. Similar bursts, but either positive or negative, can also be observed in the corresponding strain-rate curves $d\gamma/dt$. Andrade’s power law creep appears as a result of the averaging process over many of these runs, mimicking the behavior of a much bigger system. The closer is the applied stress to the threshold the longer is the collective power-law motion before the system falls either in the jammed or in the moving state. Precisely at the critical point and for the case of an infinite system, the Andrade power-law could last indefinitely.

Above the stress threshold, the system eventually exhibits a linear creep regime in which the dislocations tend to glide in a coherent manner. The dependence of the steady strain-rate value on the external shear stress is shown in Fig. 3. Within the error bars, the simulation data for the higher stress values considered can be fit quite nicely by a cubic law dependence (see the solid line in the plot). This is an interesting result since, if we were to compare with the nonlinear rheology characteristic of amorphous polymeric networks or other soft glassy materials [18], it would correspond to an effective *shear-thinning viscosity* for the dislocation ensemble which decreases with the strain-rate as $\eta = \sigma(d\gamma/dt)^{-1} \sim (d\gamma/dt)^{-2/3}$. This result is in good agreement with the theoretical results obtained in Ref. [18] and compatible with the power law shear-thinning behavior $\eta \sim \dot{\gamma}^{-\alpha}$ with $\alpha = 0.5$ –1.0 observed in many different complex fluids [5]. It also seems to satisfy the empirically established Cox-Merz rule [19]. Notice, however, that the

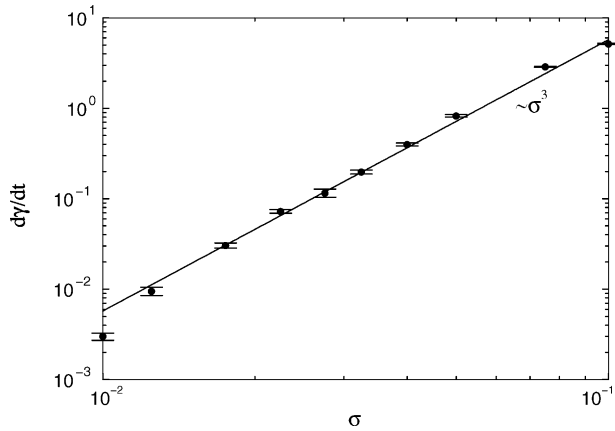


Fig. 3. Steady strain rate for different stress values in a double logarithmic scale [13]. The solid line represents a cubic dependence of the form $d\gamma/dt \sim \sigma^3$ which appears to be in good correspondence with the simulation data for the higher stress values considered.

concentration of dislocations in the crystal needs not be too high to warrant the presence of kinematical constraints and metastability in the dynamics. Here, high concentrations are replaced by the long-range character of their mutual interactions, that favor collective motions and rearrangements, and by their ability to form intricate structures that tend to glide in a coherent manner and thus can hamper their own relative motions, driving the system to a jammed state.

3. Tearing transition and plastic flow in superconducting thin films: the Corbino geometry

A vast experimental and theoretical effort has been recently devoted to characterize the phase diagram of flux lines in type II superconductors [20–22]. These quanta of magnetic flux penetrate the superconductor above a threshold value of an applied magnetic field H , the lower critical field, and their concentration increases up to the upper critical field, above which the material becomes normal. Depending on the temperature value T , H , and sample preparation, vortices can either form a crystal [23], which at higher temperatures melts into a liquid [24], or due to quenched disorder, they may exhibit more complex glassy phases [22]. Of special importance is the non-equilibrium response of vortex matter to the flow of an external current, since the dissipative motion of the vortices induces an undesirable macroscopic resistance. The moving phase can be as simple as the collective motion of an elastically deforming vortex crystal or more complex, such as in plastic vortex flow [31].

Transport experiments in superconductors are often performed in the so-called Corbino disk geometry [25–28] to efficiently override spurious effects induced by vortex motion across the sample boundaries. There a disk-shaped superconductor is placed in a magnetic field parallel to the disk axis, and a current I is injected at a metal contact in the disk center that flows radially towards the disk boundary. This

radial current generates an azimuthal Lorentz force acting on the vortices $\mathbf{f}_L(r) = \hat{\theta}\Phi_0 J(r)/c$, where Φ_0 is the quantized flux carried by the vortices, the current density inside the disk is given by $\mathbf{J}(r) = \hat{r}I/(2\pi rh)$, h is the thickness of the specimen, and c is the speed of light. Therefore, vortices tend to move in concentric circles without crossing the sample boundaries, avoiding edge contamination. The current-voltage (I - V) curve provides an indirect measure of vortex dynamics, since vortex motion induces an electric field proportional to the vortex velocities.

Vortices in the Corbino geometry exhibit intriguing dynamic phases as a function of T , H , and I . López et al. [28] have evaluated the vortex velocity profiles after measuring the voltage drop across a series of contacts placed radially on a $\text{YBa}_2\text{Cu}_3\text{O}_{7-\delta}$ disk. For low currents and temperatures all the vortices move as a rigid solid, giving rise to a linear velocity profile $v(r) = \omega r$. Above a threshold current I_0 , the vortex crystal cannot sustain the shear stress induced by the resulting inhomogeneous Lorentz force and the response becomes plastic. Finally, above the vortex lattice melting temperature T_M , the velocity profile is fluid-like and decays as $v(r) \sim 1/r$. Marchetti et al. [29] have analyzed a theoretical model of vortex flow in the Corbino geometry and interpreted the shear yielding as a dislocation unbinding transition. Plastic flow would appear as soon as the current-induced shear stress is large enough to separate an existing pair of bound dislocations.

Transport in the Corbino disk can also be studied by simulations of interacting vortices [30]. One considers a set of N rigid vortices confined in a disk of radius D . The equation of motion for each vortex i at position \mathbf{r}_i

$$\Gamma \frac{d\mathbf{r}_i}{dt} = \sum_j \mathbf{f}_{vv}(\mathbf{r}_i - \mathbf{r}_j) + \mathbf{f}_L(\mathbf{r}_i), \quad (1)$$

where Γ is an effective viscosity for vortex flow. The first term on the right hand side of this equation follows from the fact that a pair of vortices interact with each other via a long-range force $\mathbf{f}_{vv}(\mathbf{r}) = AK_1(|\mathbf{r}|/\lambda)\hat{r}$, where $A = \Phi_0^2/(8\pi^2\lambda^3)$, λ is the London penetration length, and K_1 is a first order modified Bessel function. Distances are always measured in units of λ . The last term corresponds to the current induced Lorentz-like force acting on the vortices. The N vortices are confined inside the disk by the external magnetic field and the sample edge barrier, that we model by imposing an extra normal force on the vortices of the form $\mathbf{f}_B = -g \exp[-(D-r)/r_0]/r_0\hat{r}$, with $r_0 = 0.1\lambda$ and $g/A = 1$. The coupled Eq. (1) are integrated numerically with an adaptive step size fifth-order Runge-Kutta method. We do not truncate the range of the vortex-vortex interaction since this leads to spurious fluctuations caused by the force discontinuities. We study the response of the system as a function of the applied current for different values of N , ranging from $N = 332$ to $N = 2064$, and D ($D = 18\lambda, 36\lambda, 72\lambda$).

As in the experiments, for low currents we find a linear velocity profile that corresponds to the rigid rotation of the

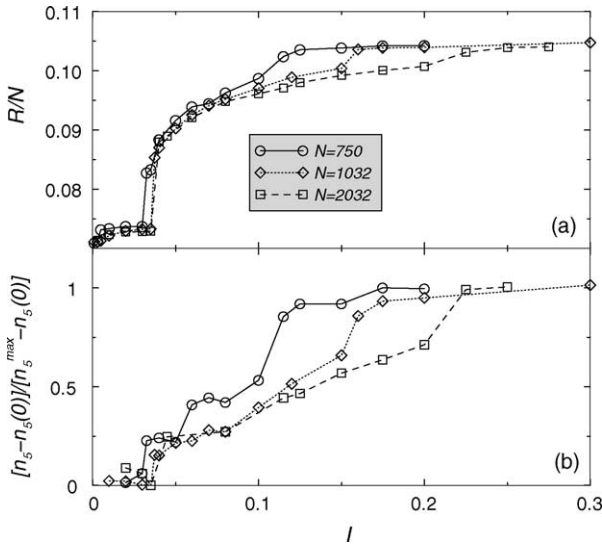


Fig. 4. The resistance and the number of vortices as a function of the current. In (a) we show the normalized resistance R/N as a function of the applied current for N vortices in a disk of radius $D = 18\lambda$. In (b) we display the excursions in the average steady number of five-fold coordinated vortices n_5 for different N is shown plotting $(n_5 - n_5(0)) / (n_5^{\max} - n_5(0))$.

vortex lattice. Above a threshold current I_0 , the profile ceases to be linear, indicating the onset of plastic flow. For higher currents $I > I_1$, we observe that vortices end up moving in uncorrelated annular channels, displaying a laminar $1/r$ velocity profile.

To better identify the transitions in the system rheology, we measure the variations of the flow resistance $R \equiv \sum_i v_i / I$ with I . After an initial transient, the resistance reaches a steady state which fluctuates strongly in the plastic regime and is much smoother in the solid and laminar phases. In Fig. 4(a) we report the steady-state resistance for different values of N and $D = 18\lambda$ as a function of I . We have normalized these curves by the corresponding number of vortices N to better visualize their characteristic features. The curves show a first sharp jump around I_0 corresponding to the breakdown of the linear velocity profile, and a smaller jump at I_1 indicating the onset of the hyperbolic profile. The final plateau scales with the number of moving vortices N . Indeed in this laminar regime, a scaling factor of N/D follows from a simple continuum approximation with a constant density of vortices.

We also construct the Delaunay triangulation of the vortex positions in the disk to characterize their topology. A pair of five-fold and seven-fold neighboring vortices identify an edge dislocation in the vortex lattice. For $I < I_0$, all vortices within the bulk of the disk are six-fold, as in a perfect triangular lattice, whereas a large number of five- and seven-fold coordinated vortices are only observed along the boundary. These are geometrically necessary dislocations and disclinations which need to be present in order to adjust a triangular lattice into a circular geometry. As the resistance, the number of five/seven-fold coordinated vortices reaches a fluctuating steady value after an initial transient. In Fig.

4(b), we report the behavior of the average steady number of five-fold vortices n_5 as a function of the current. We have subtracted the average number of geometrically necessary boundary defects $n_5(0)$, and normalized the curves by its maximum value $n_5^{\max} - n_5(0)$ to better visualize their main features. The curves reported in Fig. 4(b) closely resemble the behavior of the resistance in Fig. 4(a) with jumps at I_0 and I_1 . As the current overcomes I_0 , new dislocation pairs are nucleated, mainly within the highly strained central region. Typically we observe the reiterative formation of new dipoles that readily unbind and glide along the direction of their Burgers vector, in most cases towards the disk boundary. To accommodate the shear stress generated by the external current, the crystal should nucleate dislocations that are able to glide either radially or tangentially. Nevertheless, in the undistorted triangular lattice (when the concentration of free dislocations is low), the dislocations that are nucleated are the most elementary (with Burgers vectors along the three basic crystalline directions), and only those with \mathbf{b} almost parallel to the radial direction can easily glide over long distances due to the Peach–Koehler forces involved.

As time goes on, the dislocation flow process exhibits an erratic character since dislocation pairs at short distances may annihilate each other or react to form a new dislocation; they assist the nucleation process at intermediate distances, and may even form various metastable structures. This intricate process is reflected by the strongly fluctuating flow resistance and the non-linear velocity profile. This strong voltage noise is reminiscent of the intermittent behavior observed in plastically deforming crystals [12], and it is a fingerprint of the onset of plastic deformation in the lattice. Further increase of the current beyond $I = I_1$ results in a smoother flow, with most vortices moving in uncorrelated concentric trajectories. Here dislocation flow appears to be quite peculiar since a significant number are settled in walls (grain boundaries) oriented along the radial direction and spanning the entire disk, which tend to glide coherently in the azimuthal direction. Grain boundaries produce the necessary deformations in the crystal that allow a stationary tangential flow (see Fig. 5). Thus at and above I_1 , the rate of nucleation of new dislocations is big enough to ensure the formation and maintenance of these type of grain boundaries whose cooperative motion marks the new regime of plastic deformation.

4. Grain growth and grain boundary depinning in vortex lattices

Transport experiments in superconductors can also be performed in a strip geometry, i.e. current is injected at one side of the sample and removed at the opposite side [31,32]. This simpler geometry is often used to study the depinning transition of vortex lattices due to quenched disorder in the material. After a standard field-cooling protocol, a polycrystalline vortex phase formed by quasi-two-dimensional grain boundaries is frequently observed in vortex lattices, for instance by

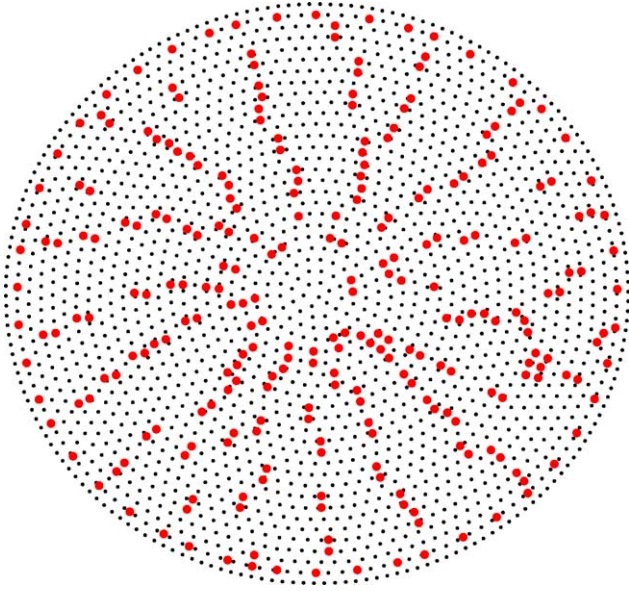


Fig. 5. Snapshot displaying dislocations in a system of $N = 2064$ vortices and disk radius $D = 36\lambda$ under an applied current $I = 0.25$. As a reference, we show all the vortex positions for a given time step. Five- and seven-fold coordinated vortices are highlighted with bigger circles.

magnetic decoration of the vortex positions [33–35,7]. Thus this geometry is suitable to perform an unusual type of grain growth experiment where the random configuration of the pinning obstacles remains constant but the properties of the lattice (namely the lattice spacing and the elastic moduli) are easily tuned with the external field applied.

Numerical simulations of a vortex polycrystal in two dimensions allow to verify and to keep track of the ordering process and the grain formation after a rapid field cooling of the vortex system. To this end, we consider a square section of linear dimension L perpendicular to the external magnetic field \mathbf{B} along the z direction, where we locate a set of N_v rigid vortices (for most of the results presented here, we have considered values of N_v ranging from 516 to 4128). The dynamics of each vortex line i at position \mathbf{r}_i can again be described by an overdamped equation of motion of the form

$$\Gamma \frac{d\mathbf{r}_i}{dt} = \sum_j \mathbf{f}_{vv}(\mathbf{r}_{ij}) + \sum_j \mathbf{f}_{vp}(\mathbf{r}_i - \mathbf{r}_j^p) + \mathbf{f}_L(\mathbf{r}_i). \quad (2)$$

The second contribution reflects the attractive interaction forces between vortex lines and quenched point defects such as oxygen vacancies or other impurities in the material. These pinning centers are randomly located at positions \mathbf{r}_i^p ($i = 1, \dots, N_p$) within the simulation box, and exert pinning forces according to a Gaussian potential of the form $V(\mathbf{r} - \mathbf{r}^p) = V_0 \exp[-(\mathbf{r} - \mathbf{r}^p)^2/\xi^2]$, whose amplitude and standard deviation are V_0 and ξ , the characteristic coherence length of the superconductor, respectively (The usual number of pinning centers N_p considered is 4128, and we have chosen $\xi = 0.2\lambda$, characteristic of low temperature superconductors such as NbSe or NbMo.) Finally, if an external current $\mathbf{J}(\mathbf{r})$ is applied to the sample, it generates a Lorentz-like force act-

ing on the vortices $\mathbf{f}_L(\mathbf{r}) = \Phi_0 \mathbf{J}(\mathbf{r}) \times \hat{z}/c$. The coupled equations of motion (2) are numerically solved imposing periodic boundary conditions in both directions.

We first consider the relaxation dynamics of the vortex lines in the absence of driving currents. Moreover, in the present analysis we completely disregard thermal effects, that is, we mimic the dynamics of the vortex system after a sudden quench of the superconducting sample from high temperatures (or equivalently, random vortex configurations) towards the lower energy states corresponding to zero temperature. After a transient regime, the dynamics gets pinned by disorder. We analyze the resulting spatial configuration of flux lines by means of Delaunay triangulations. A pair of a five-fold and a seven-fold neighboring vortices correspond to a dislocation in the vortex lattice. In the course of the simulations, the number of five-/seven-fold coordinated vortices is the same, indicating that during the relaxation process no other topological defects such as disclinations appear to be present in the lattice. Initially, there is a gradual ordering process of dislocations in grain boundaries that screens out the long range stress and strain fields created by dislocations in the lattice. The resulting polycrystalline structure evolves in time until the residual stress accumulated in the distorted lattice drops down below the critical value σ_c . At this point, grain boundaries get pinned by disorder limiting the average grain size (see Fig. 6). Moreover, the limit grain size appears to increase as the magnetic field increases $B \propto N_v$, in qualitative agreement with experimental results [7] and the theoretical predictions reported in Ref. [36].

Different experimental, or simulation, protocols will certainly influence the relaxation dynamics and the resulting metastable configurations of trapped dislocations and

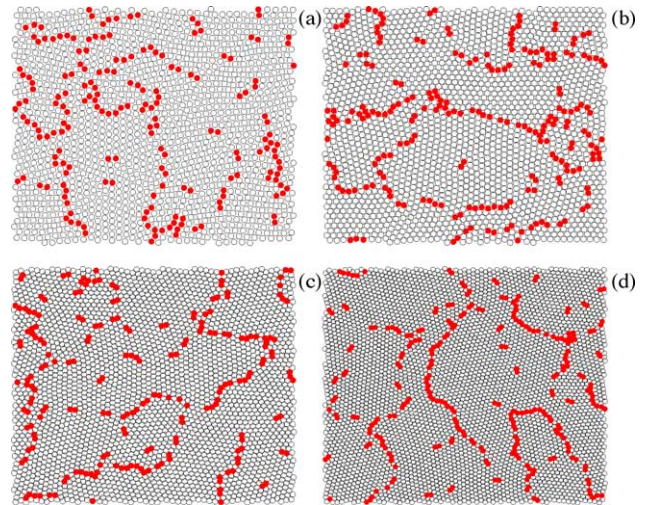


Fig. 6. Pinned vortex structure for different values of the magnetic field: (a) $N_v = 1460$, (b) $N_v = 2064$, (c) $N_v = 2919$, (d) $N_v = 4128$, after a sudden field cooling from a disordered vortex state in a simulation cell of linear size $L = 36\lambda$. The colored five-/seven-fold coordinated vortices (filled circles) indicate dislocations in the vortex lattice. The average grain size seems to grow with the intensity of the magnetic field inside the cell.

grain boundaries. Metastability and history-dependent features have been long recognized in driven vortex lattices [37]. We have considered a field-cooling procedure since most of the Bitter decoration experiments are performed in a similar manner [34,35], and can thus be well described by the current simulations. Nevertheless, other numerical protocols can also be devised, as for instance the one recently proposed in Ref. [38] to examine the vortex topology across the so-called peak-effect, that are better suited to reproduce diverse experimental conditions.

In this section, we also study the behavior of the critical current $J_c(B)$ for these vortex polycrystals by means of numerical simulations. An externally applied current may induce the annealing of the metastable configurations (at least, to a certain degree that obviously depends on its intensity) present in Fig. 6. This is indeed observed in our numerical simulations, where we can as well identify the critical current J_c below which the average motion of the vortex lattice eventually ceases after a rich initial transient of plastic flow. A small current below the threshold value $J_c(B)$ gives rise to non-trivial (i.e. not just a slight drift along the force direction f_L^x) changes of the displacement field \mathbf{u}_n of the vortex lattice. The vortex displacements are heterogeneously distributed and a small component perpendicular to the force direction is indeed observed. This in turn, implies changes of the elastic shear stress distribution responsible for the Peach-Koehler forces acting on grain boundary dislocations that, as a consequence, may move and rearrange in response to the new force field.

We have determined the dependence of the critical current on the magnetic field by carrying out simulations for different densities of vortices in the simulation cell. Moreover, we have compared these results with those corresponding to a completely different initial state: a perfect single crystal configuration with similar densities. Our results are summarized in Fig. 7. The qualitative and quantitative differences between the two curves represented in the figure are due to the presence of grain boundaries. The presence of these topological defects in the vortex configuration enhances the critical current needed to give rise to a steady regime of plastic flux flow that, in this case, appears to be controlled by grain boundary motion. Plastic flow may be mediated by the glide motion of grain boundaries and this particular mechanism may become the most relevant when the grain sizes are limited, and there is a high fraction of grain boundary atoms. According to our numerical results, grain boundaries are more efficiently pinned by disorder [36]. In both cases, we observe the decrease of J_c with an increasing density of vortices until it reaches a plateau for the largest numbers of vortices considered. The decrease observed in the polycrystalline samples seems to be reasonably well described by a power law fit of the form $J_c \sim N_v^{-0.8}$ before the plateau. It is also worth noting that we have not considered the renormalization of either the penetration length λ or the coherence length ξ of the superconductor with the intensity of the magnetic field B . Within a mean-field scenario, these parameters should diverge as the magnetic field

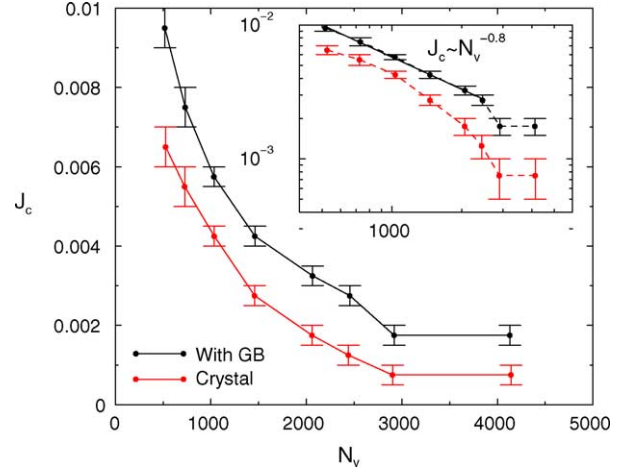


Fig. 7. The critical current J_c as a function of the number of vortices N_v in the simulation cell. The number of pinning points $N_p = 4128$, the cell size $L = 36\lambda$, and the Ginzburg–Landau parameter considered is $\kappa = 5$. The upper line shows the results obtained starting from initial field-cooled configurations containing grain boundaries, whereas the lower curve shows the results for perfect crystalline initial configurations. In the inset, we depict the same data in a double-logarithmic scale to better illustrate the qualitative differences between the two curves.

approaches the upper critical field $B_{c2} = \Phi_0/2\pi\xi$. An estimation of the reduced field values we are dealing with in the simulations yields $b = B/B_{c2} = 2\pi N_v/(\kappa^2 L^2) \sim (0.1–0.8)$. This means that the renormalization of λ and ξ will be especially relevant for the last point of the curves in Fig. 7. Recent simulations of similar vortex lattices [38] show that indeed such a field renormalization could be responsible for a sudden increase of the critical current close to the upper critical field B_{c2} .

5. Conclusions

To summarize, the flow of dislocation structures in crystalline solids undergoing plastic deformation shares common features with the rheology of soft glassy materials. Simplified dislocation dynamics models successfully capture the main qualitative properties and appear to corroborate these analogies. This suggests a possible interpretation of dislocation motion within the general *jamming* scenario that is currently being investigated to ascertain the non-equilibrium behavior of this wide class of materials.

Dislocation dynamics models appear to be particularly well suited to describe plastic flow and dislocation-induced phase transitions in vortex lattices in type II superconductors. We have shown that, in response to an injected current in the superconductor, the resistance exhibits sharp jumps indicating the onset of two different regimes of plastic flow in the superconducting Corbino disk. The first is mediated by dislocation motion, mainly along the radial direction, whereas the second is mediated by the coherent glide motion of radial grain-boundaries. We have also described the formation of

grain boundaries and vortex polycrystals in thin superconducting films with quenched disorder. Here grain boundary depinning and glide fully control the plastic flow of the lattice.

Acknowledgements

M.C.M. acknowledges financial support from the Ministerio de Educación y Ciencia, Spain.

References

- [1] J. Friedel, Dislocations, Pergamon Press, Oxford, 1967.
- [2] A.H. Cottrell, Dislocations and Plastic Flow in Crystals, Oxford University Press, London, 1953.
- [3] J.P. Hirth, J. Lothe, Theory of Dislocations, Krieger Publishing Company, 1992.
- [4] F.R.N. Nabarro, Theory of Crystal Dislocations, Dover, New York, 1992.
- [5] R.G. Larson, The Structure and Rheology of Complex Fluids, Oxford University Press, New York, 1999.
- [6] M.-C. Miguel, A. Vespignani, M. Zaiser, S. Zapperi, Phys. Rev. Lett. 89 (2002) art. no. 165501.
- [7] I.V. Grigorieva, Supercond. Sci. Technol. 7 (1994) 161; I.V. Grigorieva, Sov. Phys. JETP 69 (1989) 194.
- [8] E.N. da C. Andrade, Proc. R. Soc. London A 84 (1910) 1; E.N. da C. Andrade, Proc. R. Soc. London A 90 (1914) 329.
- [9] N.F. Mott, Phil. Mag. 44 (1953) 741.
- [10] A.H. Cottrell, Phil. Mag. Lett. 73 (1996) 35; A.H. Cottrell, Phil. Mag. Lett. 74 (1996) 375; A.H. Cottrell, Phil. Mag. Lett. 75 (1997) 301.
- [11] F.R.N. Nabarro, Phil. Mag. Lett. 75 (1997) 227.
- [12] M.-C. Miguel, A. Vespignani, S. Zapperi, J. Weiss, J.R. Grasso, Nature 410 (2001) 667.
- [13] Lengths are measured in units of y_e , the annihilation distance, time in units of $t_0 = y_e^2/(\chi_d Db^3)$, with χ_d the effective mobility of dislocations and $D = \mu/2\pi(1 - \nu)$, and stresses in units of $\sigma_0 = Db/y_e$.
- [14] A.J. Liu, S.R. Nagel, Nature 396 (1998) 21.
- [15] A.J. Liu, S.R. Nagel (Eds.), Jamming and Rheology, Taylor and Francis, London, 2001.
- [16] W.K. Kegel, A. van Blaaderen, Science 287 (2000) 290.
- [17] E. Weeks, et al., Science 287 (2000) 627.
- [18] L. Berthier, J.-L. Barrat, J. Chem. Phys. 116 (2002) 6228.
- [19] W.P. Cox, E.H. Merz, J. Polym. Sci. 28 (1958) 619.
- [20] G. Blatter, et al., Rev. Mod. Phys. 66 (1994) 1125.
- [21] E.H. Brandt, Rep. Prog. Phys. 58 (1995) 1465.
- [22] T. Giamarchi, S. Bhattacharya, C. Berthier et al. (Eds.), High Magnetic Fields: Applications in Condensed Matter Physics and Spectroscopy, Springer-Verlag, Berlin, 2002, p. 314.
- [23] A.A. Abrikosov, Zh. Eksp. Teor. Fiz. 32 (1957) 1442.
- [24] H. Safar, et al., Phys. Rev. Lett. 69 (1992) 824.
- [25] Y. Paltiel, et al., Nature 403 (2000) 398; Y. Paltiel, et al., Phys. Rev. Lett. 85 (2000) 3712.
- [26] G.W. Crabtree, et al., J. Low Temp. Phys. 117 (1999) 1313.
- [27] G. D'Anna, et al., Phys. Rev. B 54 (1996) 6583.
- [28] D. López, et al., Phys. Rev. Lett. 82 (1999) 1277.
- [29] P. Benetatos, M.C. Marchetti, Phys. Rev. B 65 (2002) 134517.
- [30] M.-C. Miguel, S. Zapperi, Nat. Mater. 2 (2003) 477.
- [31] S. Bhattacharya, M.J. Higgins, Phys. Rev. Lett. 70 (1993) 2617.
- [32] M. Marchevsky, et al., Phys. Rev. Lett. 78 (1997) 531.
- [33] M.V. Marchevsky, et al., Phys. Rev. B 57 (1998) 6061.
- [34] F. Pardo, et al., Phys. Rev. Lett. 78 (1997) 4633.
- [35] Y. Fasano, et al., Phys. Rev. B 66 (2002) 020512.
- [36] P. Moretti, M.-C. Miguel, M. Zaiser, S. Zapperi, Phys. Rev. Lett. 92 (2004) 257004.
- [37] W. Henderson, et al., Phys. Rev. Lett. 77 (1996) 2077.
- [38] M. Chandran, cond-mat/0407309 (2004).